

Short Communication

Electrochemical Analysis of Passivation Film Formation on Steel Rebar in Concrete

Xiaoyu Shang*, Youjia Zhang, Na Qu and Xiaocheng Tang

Department of Civil Engineering, Northeast Dianli University, Jilin, 132012, P.R. China

*E-mail: shangxiaoyu@nedu.edu.cn

Received: 19 March 2016 / Accepted: 14 May 2016 / Published: 4 June 2016

In this article, the passivation film of rebar was formed using cyclic voltammetry (CV) on reinforced concrete. The detail composition of the passivation film was analyzed by X-ray photoelectron spectroscopy. The electrochemical properties of the passivation film formed using the CV method were compared with the naturally formed passivation film. Study showed the properties of the passivation film could be affected by the chloride ions concentration and the electrolyte pH value. More oxidized passivation film could be formed when the presence of the chloride ions. Meanwhile, the decreasing of the pH value could enhance the content of chromium in the film and reduce the magnetite.

Keywords: Reinforced concrete; Corrosion; Cyclic voltammetry; Electrochemistry; XPS; Passivation film

1. INTRODUCTION

Carbon steel rebar is commonly used in concrete structures due to the cheap price and mature process [1]. However, carbon steel rebar corrosion has generated much concern with regard to the short service life as well as the potential safety problems. In recent years there was an accelerate desires for using stainless steel rebar instead of carbon steel rebar in the concrete structures, which could highly enhance the durability of the structures. The corrosion resistance of the stainless steel rebar is due to its surface passivation layer, which could self-regenerate and lower the corrosion process. Double layer of passivation film was commonly formed on the stainless steel rebar surface which consisted by a chromium oxide/hydroxide inner layer with an iron oxide outer layer [2, 3]. The formation of iron oxide outer layer is mainly controlled by the formation potential. For example, Fe_3O_4 and $\text{Fe}(\text{OH})_2$ are two main components of the outer layer when the formation process underwent low potential range. On the other hand, Fe_2O_3 and FeOOH are two dominate species when the formation

process underwent high potential range. Other elements also could be migrated when the formation potential shifted from low range to high range. For example, the content of the nickel will decrease in the passivation layer and the molybdenum could be enriched in the passivation film [4, 5]. The corrosion resistance performance of the passivation film could be influenced by several factors including the composition, electrochemical property and semiconductive ability [6].

Different methods have been established for analysis of the stainless steel materials [7, 8]. Among them, electrochemical approach has been found more reliable. Studies showed the successful application of an electrochemical method for analyzing passivation film formation at different materials such as iron [9, 10], carbon steel [11, 12] and stainless steel [13-15]. On the other hand, X-ray photoelectron spectroscopy analysis has been found more accurate for composition status analysis. Analysis of the passivation film on the steel rebar was very complicated because many parameters could affect its performance including temperature, oxygen content, pH condition, type of electrolyte and composition of the alloy [16].

Cyclic voltammetry (CV) is a popular method has been widely applied for growing passivation film on the steel rebar surface due to its not only results a thicker passivation film but also provides much useful information about the passivation formation reaction [17-25]. Particularly, CV provides the redox information of various electrochemical reactive species during the scan. Moreover, the influence of the electrolyte during the passivation film formation also can be determined. Not likes the open circuit potential method [26, 27], the passivation film formed using the CV method could also be affected by the setting parameters, such as scan rate and scan cycle.

In this contribution, the CV method was adopted for the formation of passivation film on a stainless steel rebar. Electrochemical studies were then carried out at different pH conditions with the presence or absence of the chloride ions. The comparison of the passivation formed using the CV method and open circuit potential method was conducted. Besides the electrochemical characterization, XPS was also applied for the detail composition analysis of the formed passivation film.

2. EXPERIMENTS

2.1. Materials

Table 1. Chemical compositions of the slag cement (all values are in wt%).

Name	CaO	SiO ₂	Al ₂ O ₃	Fe ₂ O ₃	SO ₃	MgO	K ₂ O	Alkali	Free lime	Loss on ignition
Slag cement	25.77	49.51	9.36	0.75	0.24	11.10	0.51	0.17	0.11	1.24

The reinforced concrete sample was prepared using general use slag cement. Table 1 shows the chemical compositions of the slag cement. The steel rebars (diameter 8 mm) was embedded in into the concrete. Table 2 shows the chemical compositions of the stainless steel rebar. NaOH and KOH was

used for preparing electrolyte with different pH conditions. NaCl was used for investigating the influence of chlorine ions.

Table 2. Chemical compositions of stainless steel rebar (all values are in wt%).

C	Si	Mn	Cr	Mo	Ni	Cu	P	S
27	0.03	0.16	18	3	10	0.22	0.04	0.03

2.2. Electrochemical measurement

All electrochemical measurements were performed at room temperature using a three electrode system. The rebar was used as the working electrode. A saturated calomel electrode (SCE) was used as the reference electrode. A platinum foil was used as the counter electrode. The electrolyte was firstly prepared by mixing 0.1 M NaOH with 0.1 M KOH solution to pH value of 13. Other pH electrolytes (pH 7 and 9) were prepared by dilution of above solution. In order to study the effect of the chlorides, NaCl was added to the blank alkaline solutions in order to obtain a 3% NaCl containing solution. An electrochemical workstation (Voltalab PGZ300) was used for CV scan and analysis. The CV scan range was set from -1.3 V to 0.6 V with scan rate of 1 mV/s.

2.3. XPS measurement

X-ray photoelectron spectroscopy (XPS) measurements were conducted using an AXIS Nova spectrometer (Kratos Analytical Ltd, UK), equipped with a monochromatic X-ray source (Al $K\alpha$) operating at 150 W (10 mA, 15 kV).

3. RESULTS AND DISCUSSION

We firstly investigated the difference of the passivation film formed under alkaline condition with different pH values [21, 28]. Based on the previous reports, the passivation film could be successfully formed at pH 13, which acts as a barrier between the stainless steel rebar and electrolyte [29, 30]. The CV profile showed clear formation peak of magnetite around -0.8 V, indicating the process of dissolution of the stainless steel and transition of the passivation film. The composition of the magnetite are mixed iron oxide states of Fe^{2+} and Fe^{3+} . Specifically, the magnetite consists a part of wustite (FeO) and a part of hematite Fe_2O_3 . The combination of the FeO and Fe_2O_3 dominants the passivation film which provides the significant performance towards rebar corrosion protection.

Figure 1A shows the CV profiles of passivation films formation at pH values of 9, 11 and 13 in the absence of NaCl. Clear peak shifts were observed on the CV scans when the pH condition decreasing, which is in a good agreement with the Pourbaix diagrams explanation [31]. Moreover, the peak intensities also showed decline, suggesting the degree of the formed passivation film decreased at

the lower pH condition. Therefore, the formation of magnetite was less efficient under low pH conditions. This observation was in good agreement with other reports [32, 33]. Moreover, as shown in the figure, the partial oxidation of magnetite was also observed on the CV profiles with an overlapping of the transition process between magnetite and maghemite oxide. The exact formation equations can be described as follow:



On the other hand, the current intensity of the chromium oxidation was increased under low pH condition, suggesting the content of the chromium in the formed passivation film enriched at low pH condition. Besides, several characteristics also need to be pointed out. The oxidation of nickel was observed on the study only at pH value of 13. This phenomenon was observed by Abreu and co-workers as well [21]. The reduction of nickel was also observed during the scan. The peaks located at -0.63 V and -1.22 V can be assigned to the reduction process of Ni_3O_4 to NiO and NiO to metallic Ni .

Figure 1B shows the CV profile of passivation films formation at pH value of 13 with 3% NaCl. It can be seen that the addition of NaCl largely increased the passive range. The intensity of the peaks current showed significant elevation, suggesting the formation of a thicker passivation layer. Compare with the Figure 1A, similar peaks were observed, indicating the composition substances had no change. No extra peak was observed on the scan, suggesting no pitting corrosion occurred during the passivation formation process with the addition of chlorine. Therefore, the formation of a passivation film could be effectively enhance the corrosion resistance of the steel rebar at alkaline condition. Another significant change after addition of NaCl is the surface area of the reverse scan was much less than the forward scan, which is commonly observed when a thicker passivation film formation [34]. We further studied the corrosion resistance performance of formed passivation film under more aggressive environment. No clear pitting corrosion could be observed on the CV scan when the pH value of the electrolyte at 11 or 9.

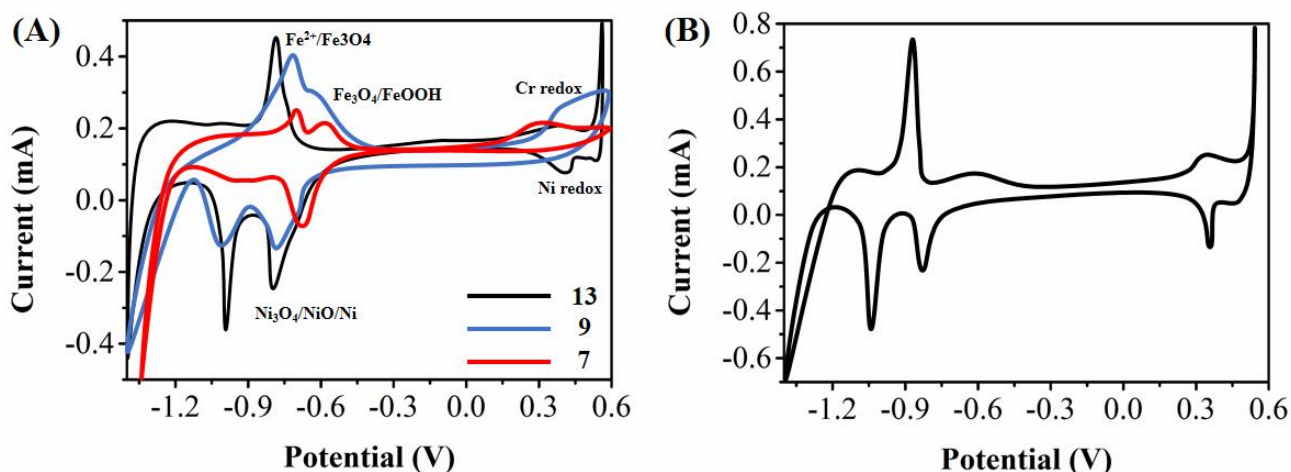


Figure 1. (A) CV scans of the passivation film formation at pH condition of 9, 11 and 13. (B) CV scan of the passivation film formation at pH 13 with 3% NaCl. Scan rate: 1 mV/s.

XPS was used for analyzing the chemical composition of the passivation film. Open cycle potential method was adopted as a control group for comparison purpose. The passivation films formed using both methods were mainly composed by iron, chromium and nickel, which are consisted with the CV profile. As reported by the other research groups [28, 35], the passivation film formed using CV method commonly thicker than that of the passivation film formed using open cycle potential method. Figure 2 shows the Fe2p3 XPS narrow scan spectra of the passivation films formed using CV and open cycle potential method. It can be seen that the metallic iron signal (around 707.1 eV) was significantly decreased in the passivation film formed using the CV method. In contrast, a clear Fe⁰ signal could be observed on the spectrum of the passivation film formed using open cycle potential method. For spectrum of the passivation film formed using CV method, peak energies corresponding to Fe₂O₃ and Fe(OH)₃/FeOOH were clearly recorded. Therefore, the composition of the passivation film formed using CV method had significant differences comparatively to the film formed using open cycle potential method. The signals of the Fe²⁺ and Fe³⁺ were much weaker at the passivation film formed using open cycle potential method than that of the film formed using CV way.

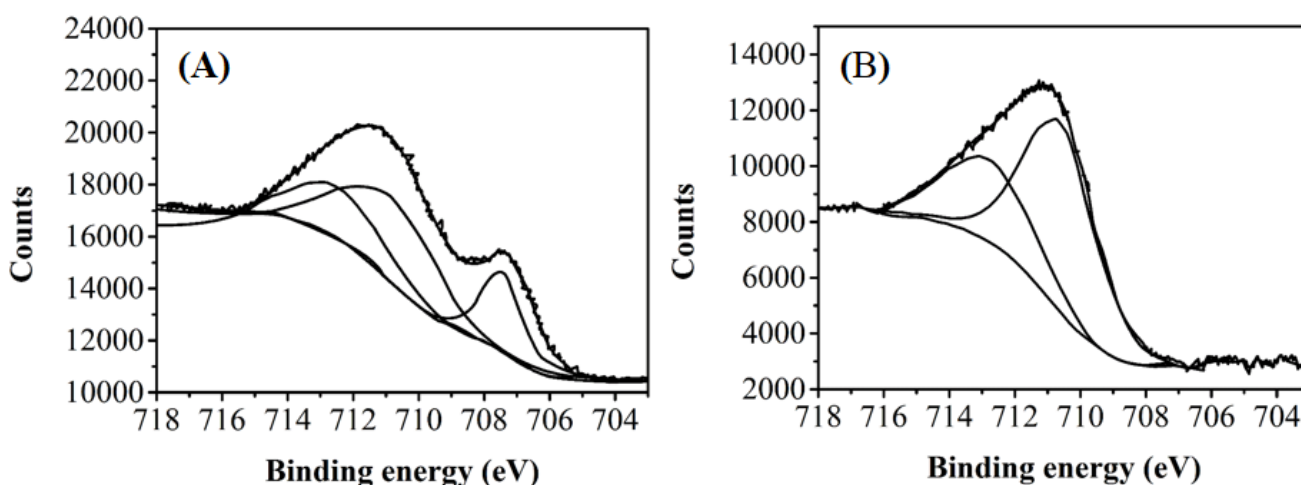


Figure 2. Fe2 p3 narrow XPS scans of the passivation films formed using (A) open cycle potential method and (B) CV method at pH 13 with 3% NaCl.

Figure 3 shows the Fe³⁺ to total of oxidized cations ratio, Fe²⁺ to Fe³⁺ ratio, Cr³⁺ to total oxidized cations ratio and Ni²⁺ to total oxidized cations ratio at passivation film formed using CV method and open cycle potential method with different pH conditions. The presence of the peak corresponded to the Fe²⁺ was recorded at passivation films formed at pH 9 and 11, indicating the Fe³⁺ outer layer of the passivation film was thinner than the film formed at pH 13. However, the amount of them still much lower than that of the passivation film formed using open cycle potential method at pH 13 electrolyte. As shown in the figure, the Fe²⁺ to Fe³⁺ ratio of the passivation films formed using CV method at pH 9 and 11 is much higher than the one formed using open cycle potential method. It worth noting that the Fe²⁺ to Fe³⁺ ratio cannot be detected due to the thicker Fe³⁺ outer layer formed at pH 13, which hidden the signal of the Fe²⁺ from the inner layer [36]. The Cr³⁺ content in the passivation films formed using two methods also had clear differences. As shown in the figure, the

amount of the detected oxidized chromium are lower for the films formed by CV. According to the previous reports, the content of the oxidized Cr usually increases when the pH value decreases [32]. The possible explanation can be the oxidized Cr hidden at inner layers of the passivation film, which cannot be able to fully detected by XPS. Moreover, the presence of the Ni species cannot be detected at the passivation film formed using CV method at pH 13 probably due to the same reason. On the other hand, the presence of the Ni species was observed at passivation layer formation at pH 9 and 11 can be ascribed to the thinner passivation layer formation.

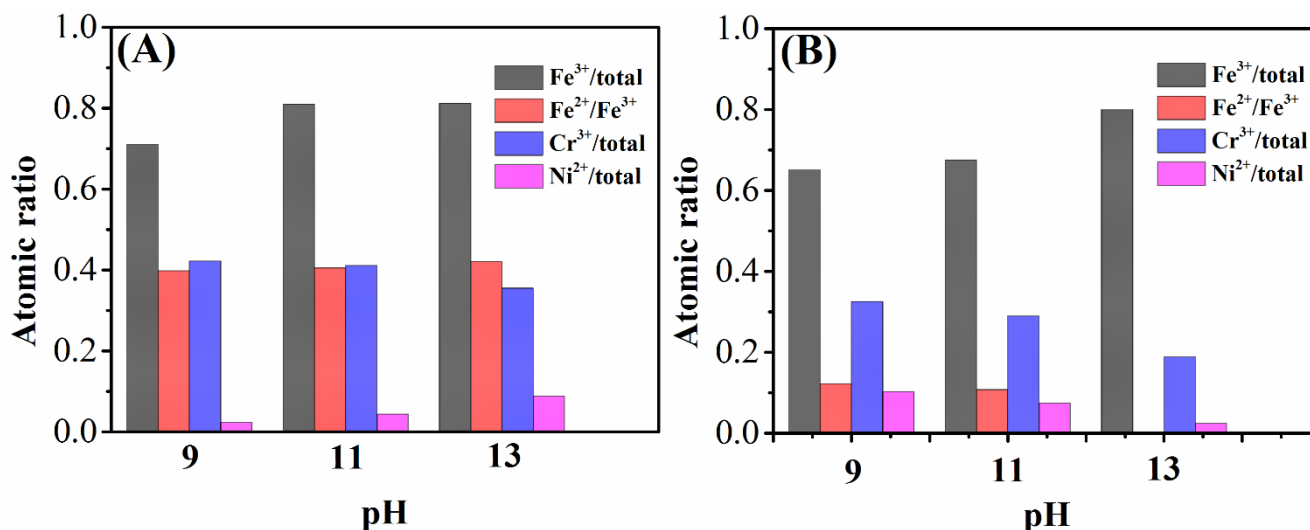


Figure 3. Comparison of Fe³⁺ to total of oxidized cations ratio, Fe²⁺ to Fe³⁺ ratio, Cr³⁺ to total oxidized cations ratio and Ni²⁺ to total oxidized cations ratio at passivation films formed at different pH condition using (A) open cycle potential method and (B) CV method.

4. CONCLUSION

Summarizing, in order to enhance the corrosion resistance performance of the concrete, CV and open cycle potential method were used for generating passivation film on stainless steel rebar. CV and XPS were used for analyzing the passivation formation process and chemical composition analysis, respectively. Result showed the CV method could yield a thicker passivation film than that of the one formed using open cycle potential method. The outer layer of the passivation film formed using the CV method enriched Fe³⁺ species while depleted in Fe²⁺ and oxidized chromium and nickel.

References

1. L. Bertolini, F. Bolzoni, T. Pastore and P. Pedferri, *British Corrosion Journal*, 31 (1996) 218
2. A. Di Paola, *Electrochimica Acta*, 34 (1989) 203
3. M.D.C. Belo, N. Hakiki and M. Ferreira, *Electrochimica Acta*, 44 (1999) 2473
4. K. Sugimoto and Y. Sawada, *Corrosion Science*, 17 (1977) 425
5. M. Montemor, A. Simões, M. Ferreira and M.D.C. Belo, *Corrosion science*, 41 (1999) 17

6. C. Rangel, T. Silva and M. da Cunha Belo, *Electrochimica acta*, 50 (2005) 5076
7. G. Qiao, Y. Hong, G. Sun and O. Yang, *Sensors Journal, IEEE*, 13 (2013) 1141
8. X. Zhao, Y. Cui, H. Wei, X. Kong, P. Zhang and C. Sun, *Smart Materials and Structures*, 22 (2013) 065014
9. H. Zhang and S.M. Park, *Journal of the Electrochemical Society*, 141 (1994) 718
10. C.M. Abreu, A. Covelo, B. Díaz, L. Freire, X.R. Nóvoa and M.C. Pérez, *Journal of the Brazilian Chemical Society*, 18 (2007) 1158
11. M. Montemor, A. Simoes and M. Ferreira, *Cement and Concrete Composites*, 25 (2003) 491
12. L. Freire, X. Nóvoa, M. Montemor and M. Carmezim, *Mater. Chem. Phys.*, 114 (2009) 962
13. M. Carmezim, A. Simoes, M. Montemor and M.D.C. Belo, *Corrosion Science*, 47 (2005) 581
14. T.S.L. Wijesinghe and D. Blackwood, *Appl. Surf. Sci.*, 253 (2006) 1006
15. J. Macák, P. Sajdl, P. Kučera, R. Novotný and J. Vošta, *Electrochimica acta*, 51 (2006) 3566
16. C.-O. Olsson and D. Landolt, *Electrochimica acta*, 48 (2003) 1093
17. N. Ramasubramanian, N. Preocanin and R. Davidson, *Journal of The Electrochemical Society*, 132 (1985) 793
18. L. Veleva, M.A. Alpuche-Aviles, M.K. Graves-Brook and D.O. Wipf, *Journal of Electroanalytical Chemistry*, 537 (2002) 85
19. J.-B. Lee and S.-W. Kim, *Mater. Chem. Phys.*, 104 (2007) 98
20. A. Kocijan, Č. Donik and M. Jenko, *Corrosion science*, 49 (2007) 2083
21. C. Abreu, M. Cristóbal, R. Losada, X. Nóvoa, G. Pena and M. Pérez, *Electrochimica Acta*, 49 (2004) 3049
22. L. Fu, G. Lai, P.J. Mahon, J. Wang, D. Zhu, B. Jia, F. Malherbe and A. Yu, *RSC Advances*, 4 (2014) 39645
23. L. Fu, G. Lai and A. Yu, *RSC Advances*, 5 (2015) 76973
24. L. Fu, S. Yu, L. Thompson and A. Yu, *RSC Advances*, 5 (2015) 40111
25. G. Lai, H. Cheng, C. Yin, L. Fu and A. Yu, *Electroanalysis*, (2015)
26. Y. González-García, G. Burstein, S. González and R. Souto, *Electrochemistry Communications*, 6 (2004) 637
27. L. Li and A. Sagues, *Corrosion*, 57 (2001) 19
28. L. Veleva, M. Alpuche-Aviles, M. Graves-Brook and D. Wipf, *J. Electroanal. Chem*, 537 (2002) 85
29. R.S. Guzman, J. Vilche and A. Arvia, *Electrochimica Acta*, 24 (1979) 395
30. S. Joiret, M. Keddám, X. Nóvoa, M. Pérez, C. Rangel and H. Takenouti, *Cement and Concrete Composites*, 24 (2002) 7
31. M. Pourbaix, N. de Zoubov and J. Van Muylder, Atlas d'équilibres électrochimiques, Gauthier-Villars Paris 1963.
32. L. Freire, M. Carmezim, M.a. Ferreira and M. Montemor, *Electrochimica Acta*, 55 (2010) 6174
33. L. Freire, M. Carmezim, M. Ferreira and M. Montemor, *Electrochimica Acta*, 56 (2011) 5280
34. B. Díaz, S. Joiret, M. Keddám, X. Novoa, M. Pérez and H. Takenouti, *Electrochimica acta*, 49 (2004) 3039
35. L. Veleva, M.A. Alpuche-Aviles, M.K. Graves-Brook and D.O. Wipf, *Journal of Electroanalytical Chemistry*, 578 (2005) 45
36. C. Abreu, M. Cristóbal, R. Losada, X. Nóvoa, G. Pena and M. Pérez, *Journal of electroanalytical chemistry*, 572 (2004) 335